DOI: 10.1002/chem.201100478

Helical Carbon Nanotubes: Intrinsic Peroxidase Catalytic Activity and Its Application for Biocatalysis and Biosensing

Rongjing Cui,[a, b] Zhida Han,[b] and Jun-Jie Zhu*[a]

Abstract: A combined hydrothermal/hydrogen reduction method has been developed for the mass production of helical carbon nanotubes (HCNTs) by the pyrolysis of acetylene at 475 °C in the presence of Fe_3O_4 nanoparticles. The synthesized HCNTs have been characterized by high-resolution transmission electron microscopy, scanning electron microscopy, X-ray diffraction analysis, vibrating sample magnetometry, and contact-angle measurements. The as-prepared helical-structured carbon nanotubes have a large specific surface area and high peroxidase-like activity. Catalysis was found to follow Michaelis–Menten kinetics and the HCNTs showed strong affinity for both H_2O_2 and 3,3′,5,5′,-tetramethylbenzidine (TMB). Based on the high activity, the HCNTs were firstly used to develop a biocatalyst and amperometric sensor. At pH 7.0, the constructed amperometric sensor showed a linear range for the detection of H_2O_2 from 0.5 to 115 μM with a correlation coefficient of 0.999 without the need for an electron-transfer mediator. Because of their low cost and high stability, these novel metallic HCNTs represent a promising candidate as mimetic enzymes and may find a wide range of new applications, such as in biocatalysis, immunoassay, and environmental monitoring.

Keywords: biosensors · enzyme catalysis · helical carbon nanotubes · nanoparticles · peroxidase nanomimetics

Introduction

Nanomaterials, especially functional nanomaterials, have received tremendous interest for biomedical and biosensing applications because of their unique optical and electrical properties, large specific surface areas, and fascinating catalytic activities.[1–8] Intriguingly, recent studies have shown that some nanomaterials have an intrinsic enzyme mimetic activity similar to that found in natural peroxidases. Fe_3O_4 was previously regarded as being biologically and chemically inert. However, Gao et al. reported that Fe_3O_4 nanoparticles (NPs) have an intrinsic enzyme mimetic activity similar to that of natural peroxidases.[9] Wei et al. made use of this novel property of Fe_3O_4 NPs as a peroxidase mimetic to detect H_2O_2 and glucose. It was concluded that the peroxidase-like activity originated mainly from ferrous ions at the surface of Fe_3O_4 NPs. The mechanism may be akin to that of the Fenton reaction.[10] Recently, Qu et al. reported that SWNTs and carboxyl-modified graphene oxide display intrinsic peroxidase-like activity, such that they can catalyze reaction of the peroxidase substrate 3,3′,5,5′,-tetramethylbenzidine TMB in the presence of H_2O_2 to produce a blue color. The results clearly showed that the observed "catalytic" effect could be attributed to the intrinsic properties of these materials rather than any metal residues.[11] Subsequently, sheet-like FeS nanostructures and spherical CeO_2 NPs were also found to display peroxidase- or oxidase-like activity, which could be used in biodetection.[12,13] In comparison with natural enzymes, the nanomaterials family may represent promising candidates for enzyme mimetics, having the advantages of controlled synthesis at low cost, tunable catalytic activities, and a high stability against harsh reaction conditions.[14] Therefore, the synthesis of artificial peroxidases with good catalytic properties and a wide range of practical applications is becoming a significant field.

Helical carbon nanotubes (HCNTs) were first predicted in 1993 by Itoh et al. and were first observed in 1994 by Zhang et al.[15,16] Since then, scientists have directed much effort towards studies of the morphology and physical characteristics of carbon nanohelices, and have suggested potential applications due to their helical structure and unique physical properties.[17,18] For example, because of their special electromagnetic (EM) properties, carbon nanohelices can be used in micromagnetic sensors, mechanical microsprings or actuators, highly elastic electroconductors, good EM wave absorbers, and so forth.[19–22] Additionally, compared with other carbon-based nanomaterials such as carbon nanotubes (CNTs), HCNTs possess specific helical structures, increased surface area, and more importantly, encapsulate a certain amount of ferromagnetic iron species,

[a] Dr. R. Cui, Prof. J.-J. Zhu
Key Laboratory of Analytical Chemistry for Life Science (MOE)
School of Chemistry and Chemical Engineering
Nanjing University, Nanjing 210093 (P.R. China)
Fax: (+86) 25-83597204
E-mail: jjzhu@nju.edu.cn

[b] Dr. R. Cui, Dr. Z. Han
Jiangsu Laboratory of Advanced Functional Materials
Changshu Institute of Technology
Changshu 215500 (P.R. China)

Supporting information for this article is available on the WWW under http://dx.doi.org/10.1002/chem.201100478.

which may favor electron transfer and facilitate catalytic activity. These features have inspired us to explore: 1) whether HCNTs can serve as potential peroxidase or oxidase mimetics, and 2) if so, how the problem of their poor solubility in common solvents may be overcome. Considering the limited number of reports in this new emerging field, further exploration was clearly required.

In previous reports, several strategies have been proposed to increase the solubility of CNTs in aqueous media. Some of them relied on dispersion in different solvents, such as strongly acidic solutions,[23] *N*,*N*-dimethylformamide (DMF),[24] Nafion,[25] and polyethyleneimine (PEI).[26] Here, we make use of a novel method of functionalizing HCNTs with poly(allylamine hydrochloride) (PAH) for biocatalysis and biosensing. In this method, the HCNTs retain their strong magnetic properties and have good solubility and dispersibility in water.

H_2O_2 is a major reactive oxygen species in living organisms, and its overproduction is implicated in the development of numerous inflammatory diseases, such as atherosclerosis, chronic obstructive pulmonary disease, and hepatitis. Furthermore, as a product of many enzyme-catalyzed reactions, H_2O_2 can serve as an indicator in monitoring quantities of biologically important molecules such as glucose.[27] Therefore, study of the catalytic reaction of HCNTs with H_2O_2 might offer a promising application in the design of HCNTs-based biosensors.

Herein, we present a new method for the synthesis of HCNTs by pyrolysis of acetylene at 475 °C in the presence of Fe nanoparticles derived from a combined method of hydrothermal fabrication and hydrogen reduction. The as-prepared HCNTs showed an attractive intrinsic peroxidase-like activity, which was found to follow Michaelis–Menten kinetics, and also showed a strong affinity for both H_2O_2 and TMB. Also, this H_2O_2 sensor showed a more sensitive response than those of enzyme-based biosensors.[28,29] To the best of our knowledge, this is the first report concerning the application of the intrinsic peroxidase-like activity of HCNTs. This study should provide new insights into the utilization of this peroxidase-like activity of HCNTs.

Results and Discussion

Characterization of the as-synthesized catalysts: To generate the catalyst, Fe_3O_4 nanoparticles (NPs) as catalyst precursor were reduced in hydrogen at 425 °C for 4 h. A scanning electron microscopy (SEM) image of the Fe_3O_4 NPs revealed a large amount of spherical NPs. The NPs were uniform in size, with an average diameter of about 50 nm, as shown in Figure 1a. The crystal structure of these nanospheres was studied by X-ray diffraction (XRD) analysis. As shown in Figure 1b, all diffraction peaks and positions matched well with those from the JCPDS card (No. 75-0033) for cubic magnetite and well-resolved diffraction peaks revealed good crystallinity of these nanospheres.[30] The results of XRD analysis confirmed that the as-synthesized catalyst was

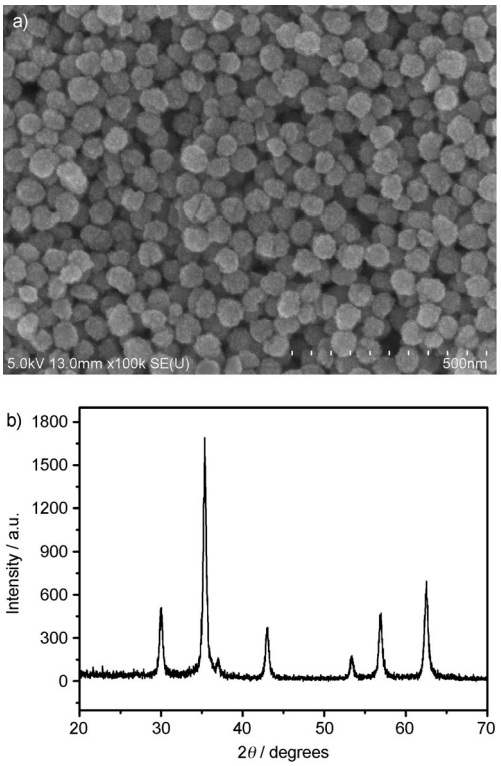

Figure 1. a) Typical SEM image and b) XRD results of the catalyst.

Fe_3O_4. Interestingly, it was found that the size of the Fe_3O_4 NPs could be easily controlled by changing the amount of NaOH.

Preparation and characterization of the HCNTs: In a previous report, Tang et al. described the synthesis of HCNTs by the pyrolysis of acetylene at 475 °C over iron NPs generated by means of a combined sol–gel/reduction method.[22] In the present work, an effective catalyst has been designed for the efficient synthesis of HCNTs based on the accumulated research in this area. We have fabricated powder Fe_3O_4 NPs catalyst by a hydrothermal method. HCNTs have been synthesized by thermal chemical vapor deposition (CVD) using Fe_3O_4 NPs as catalyst. It is noteworthy that the hydrothermal method used in these studies makes it possible to prepare high-quality powder catalysts in large quantities, in a simple way and at low cost.

Figure 2a shows an SEM image of the as-prepared HCNTs sample. Double-HCNT structures are clearly visible. The tubes range from 150 to 200 nm in diameter, which is larger than the dimension of previously reported HCNTs.[19] Most tubes are coiled in a regular and tight fashion with a very short coil pitch. SEM and transmission electron microscopy (TEM) investigation revealed that these nanotubes always present a symmetrical growth mode, that is, they are always in the form of twin helices. A closer examination revealed that the two helical nanotubes were mirror images of each other, as shown in Figure 2b. They exhibit identical cycle (or turn) numbers, tube diameters, coil diameters, coil

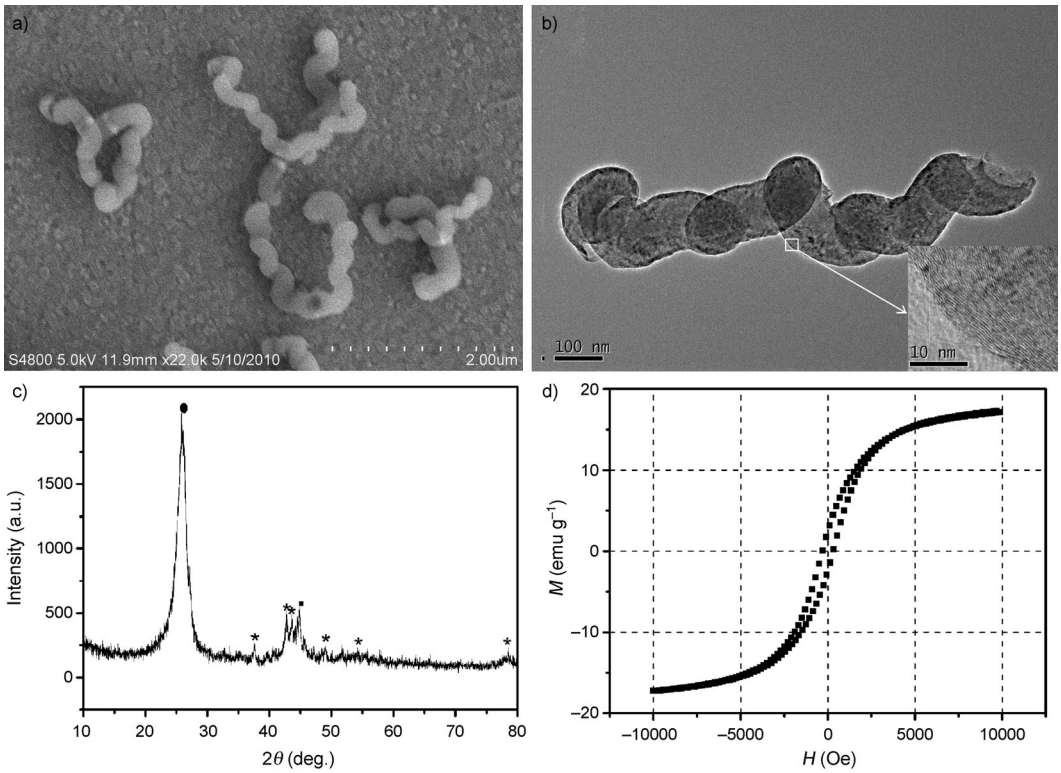

Figure 2. a) Typical SEM image, b) TEM image, c) XRD (● = graphite, ■ = α-Fe, and ∗ = Fe_3Cl), and d) magnetization curve of the HCNTs. Inset: HR-TEM image of the HCNTs.

lengths, and coil pitch, but are of opposite helical sense. The high-resolution transmission electron microscopy (HRTEM) image in the inset of Figure 2b shows the graphitic layers and the structural disorder of graphite in the HCNTs. This is reflective of the relatively low growth temperature (475 °C).

The XRD pattern of the as-prepared HCNTs sample is shown in Figure 2c. The diffraction peaks can be indexed to phases of graphite, α-Fe, and Fe_3C, a clear indication of the formation of Fe_3C from Fe and carbon in the synthesis of the HCNTs. Figure 2d shows the magnetization curve (M vs. H) for the HCNTs sample measured at 300 K. The saturation magnetization (M_S) and the coercivity (H_c) of the as-prepared sample were 17.1 emu $g^{-1}$and 310.2 Oe, respectively. Inductively coupled plasma (ICP) spectrometry analysis showed that the Fe content in the sample was 12.3 wt %. Given that Fe_3C is the major Fe-containing phase in the as-prepared sample (as revealed by XRD studies, Figure 2c), the amount of Fe_3C in the sample was deduced to be about 13.2 wt %. Based on the Fe_3C content and the fact that the magnetization of Fe_3C is about 128 emu g^{-1} at 300 K, we estimate that the saturation magnetization of the sample should be around 16.9 emu g^{-1}, which is close to the value of 17.1 emu g^{-1} observed experimentally.

To investigate the influence of catalyst size on carbon production, Fe_3O_4 NPs with diameters of 80 and 110 nm were used as catalyst precursors, and the corresponding carbon products are designated as m-HCNTs and l-HCNTs, respectively. ICP spectrometry results indicated that the amounts of Fe in the samples of m-HCNTs and l-HCNTs were 8.6 and 6.3 wt %, respectively. HR-TEM and SEM images of HCNTs, m-HCNTs, and l-HCNTs are shown in Figure S1 (in the Supporting Information). One can see that the yield of helical structures was lower than that of HCNTs. For m-HCNTs and l-HCNTs, carbon species with straight and irregular morphologies were the major products. It is clear that the average diameter of the helical structured tubes was smaller than that of the straight form. Therefore, one can deduce that the size of the Fe_3O_4 NPs has a determining effect on the yield and selectivity for HCNTs, with small Fe_3O_4 particles favoring the growth of HCNTs with relatively low yield, whereas large particles favor the growth of the straight form with high yield. Similar phenomena have also been noted in previous reports.[22,31]

Although HCNTs have been prepared for many years, to the best of our knowledge, their application in bioassay has not hitherto been reported. One possible reason may be their poor solubility in water. In previous reports, carbon nanomaterials have generally been treated with a mixture of concentrated sulfuric and nitric acids to increase their solubility in aqueous media.[23] Here, we report for the first time the method of functionalizing HCNTs with poly(allylamine hydrochloride) (PAH), which renders them soluble and dispersible in water while retaining their strong magnetic properties.

The functionalization process of the HCNTs with PAH was monitored by microelectrophoresis measurements (ex-

pressed as a ξ-potential). As expected, the original HCNTs in aqueous solution (pH 7.0) had a negative ξ-potential of −16.5 mV. Thus, the prepared HCNTs were negatively charged and were electrostatically attracted to the cationic polyelectrolyte PAH, which provided a homogeneous distribution of positive charges. The presence of an adsorbed layer of positively charged PAH on the HCNTs caused a reversal in ξ-potential to a positive value (+48.5 mV).

Contact-angle measurements were carried out to investigate the change in the surface properties of the HCNTs after their functionalization with PAH. As shown in Figure 3a and b, the HCNTs and PAH-functionalized HCNTs showed water contact angles of 145.5 and 28.5°, respectively. The PAH-functionalized HCNTs showed a lower contact angle, indicating good dispersion in water, which provides a great opportunity for their application in bioassays.

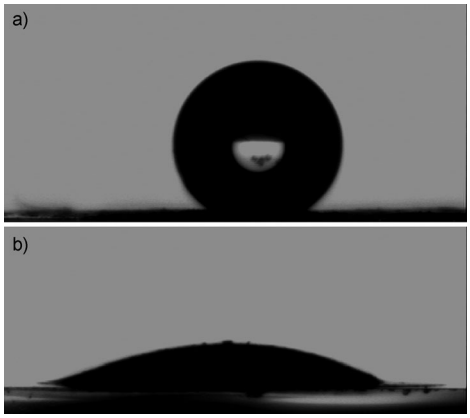

Figure 3. Contact angles of a) HCNTs and b) PAH-functionalized HCNTs.

Peroxidase-like activity of HCNTs: It is well known that peroxidase can catalyze the oxidation of a peroxidase substrate to produce a color change. To investigate the peroxidase-like activity of the PAH-functionalized HCNTs, similar experiments were carried out. A black solution of HCNTs could catalyze the oxidation of a peroxidase substrate, TMB, by H_2O_2 to produce a blue color, as shown in the inset in Figure 4. The resulting solution showed a maximum absorbance at 652 nm, which originated from the oxidation product of TMB. As shown in Figure 4, no such absorption spectrum was observed from a solution in the absence of HCNTs. When HCNTs were added to the solution, the absorption maximum at 652 nm appeared as a strong response. Similar to peroxidase, the catalytic activity of HCNTs is dependent on pH and temperature (see Figure S2 in the Supporting Information). Under our experimental conditions, the optimal pH and temperature were identified as 4.0 and 40 °C, respectively.

Steady-state kinetics: The apparent steady-state kinetic parameters for the reaction were determined at 40 °C when HCNTs were employed as the catalytic agent. Absorbance

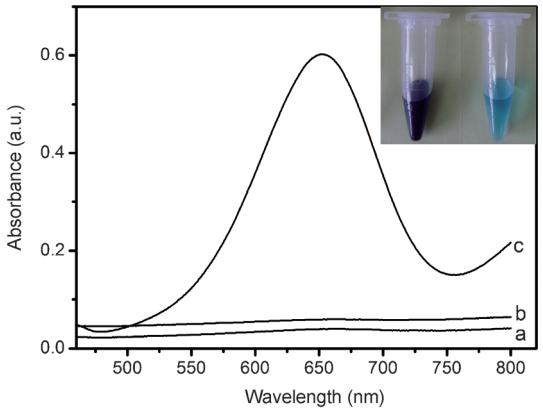

Figure 4. Typical absorption curves of TMB reaction solutions catalytically oxidized by the HCNTs in the presence of H_2O_2 incubated at 40 °C in pH 4.0 buffer: a) 500 mM H_2O_2 without HCNTs, b) 0 mM H_2O_2 with HCNTs, c) 100 mM H_2O_2 with HCNTs. Inset: Images of the solutions of HCNTs (left) and the mixture of TMB and H_2O_2 after catalytic reaction by HCNTs (right).

data were back-calculated to concentration by the Beer–Lambert Law using a molar absorption coefficient of 39 000 $M^{-1}cm^{-1}$ for TMB-derived oxidation products.[34]

Apparent steady-state reaction rates at different concentrations of substrate were obtained by calculating the slopes of initial absorbance changes with time. The curves shown in Figure 5 indicate that the reaction catalyzed by HCNTs displayed Michaelis–Menten kinetics. Michaelis–Menten constants (K_m) were obtained from Lineweaver–Burk plots.[9,35] The apparent K_m value for HCNTs with TMB was 0.020 mM, while the apparent K_m value for horseradish peroxidase (HRP) with H_2O_2 was 0.4 mM. The latter coincides with that reported in the literature.[9] The twenty-times lower K_m value of the HCNTs compared with that of HRP suggests that they have a significantly higher affinity for TMB than HRP.

On the other hand, the apparent K_m value of the HCNTs with H_2O_2 was 41.42 mM, significantly higher than that of 3.7 mM for HRP in solution. Nevertheless, the apparent K_m value was three times lower than that of 154 mM for Fe_3O_4 NPs,[9] indicating a better affinity of the HCNTs for H_2O_2 compared with that of Fe_3O_4 NPs.

As a catalytic agent, HCNTs exhibited similar catalytic efficiency to that of HRP. To examine whether the peroxidase activity of HCNTs depends on the amount of iron, we compared the catalytic activities of HCNTs, m-HCNTs, and l-HCNTs containing different amounts of iron. ICP spectrometry results indicated that the amounts of Fe in these samples were 12.3, 8.6, and 6.3 wt%, respectively. The HCNTs showed different levels of activity towards TMB in the order HCNTs > m-HCNTs > l-HCNTs, as shown in Figure 6, that is, the higher the Fe content, the higher the catalytic activity. This phenomenon may be due to the greater amount of Fe providing more catalytic centers to interact with the substrate. It was important to rule out the possibility that the observed activity was caused by leaching of iron ions

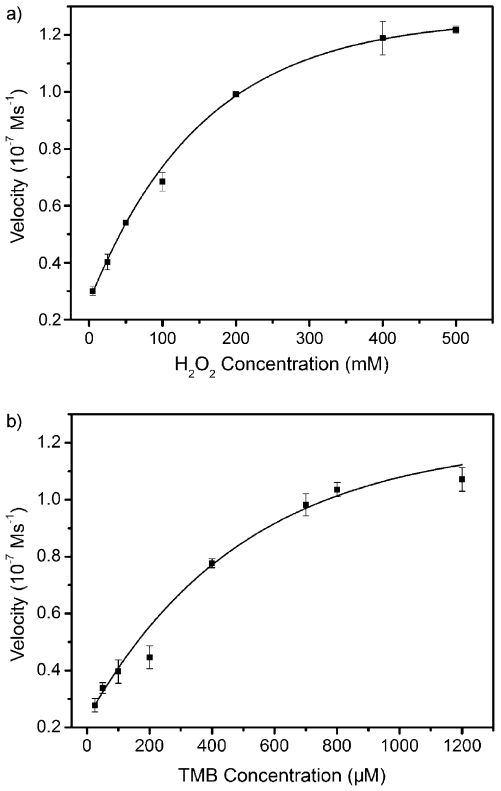

Figure 5. Kinetic analysis for HCNTs with a) H_2O_2 and b) TMB as substrates, respectively. The velocity of the reaction was measured using 40 μg mL^{-1} HCNTs (a, b) in 500 μL of 25 mM Na_2HPO_4 of pH 4.0 at 40 °C. The concentration of TMB was 800 μM and the H_2O_2 concentration was varied (a); the concentration of H_2O_2 was 500 mM and the TMB concentration was varied (b).

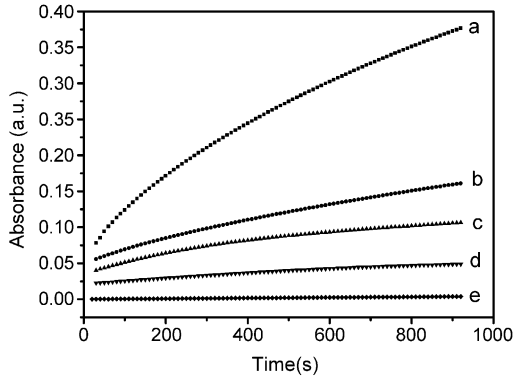

Figure 6. Time-dependent absorbance changes at 652 nm in the presence of HCNTs (a), m-HCNTs (b), l-HCNTs (c), MWCNTs (d), and the remaining solution after removal of the HCNTs, which were incubated in the pH 4.0 reaction buffer for 10 min at 40 °C (e).

into the acidic solution. To test this, we incubated HCNTs in the standard reaction buffer (pH 4.0) for 10 min and then removed them from the solution with a magnet. We then compared the activity of the leachate with that of the HCNTs under the same conditions. As shown in Figure 6e, the leachate showed no activity, confirming that the observed peroxidase-like activity was due to intact HCNTs. More importantly, we compared the catalytic efficiencies of HCNTs and multi-walled carbon nanotubes (MWCNTs). The results clearly showed that the HCNTs had better catalytic performance than the MWCNTs under the same experimental conditions.

Electrocatalytic activity of HCNTs in the reduction of H_2O_2: We applied HCNTs in the fabrication of an electrochemical sensor to detect H_2O_2. It is well known that the accurate and rapid determination of H_2O_2 is of practical importance in bioanalytical and environmental fields.[36] A large number of enzyme-based biosensors have been developed for the detection of H_2O_2, but the enzymes were relatively expensive and their function was critically dependent on environmental conditions.[37,38] Furthermore, due to their inherent instability, enzymes clearly cannot provide biosensors with long-term stability.[39] On the contrary, HCNTs could be an excellent substitute for peroxidase enzymes.

The amperometric response of an HCNTs-modified glassy carbon electrode (HCNTs/GCE) to H_2O_2 is shown as curve a in Figure 7. Upon addition of an aliquot of H_2O_2 to

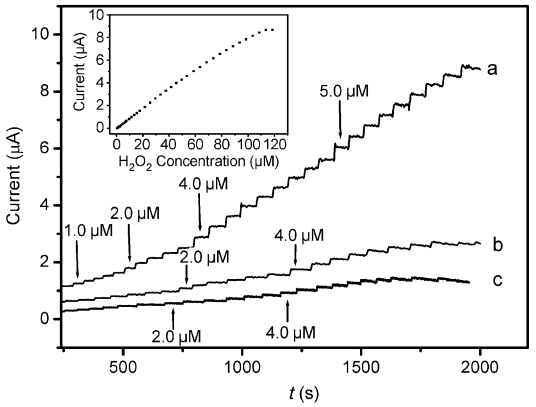

Figure 7. Amperometric responses of GCEs modified with HCNTs (a), l-HCNTs (b), and MWCNTs (c) at −0.40 V upon successive additions of H_2O_2 to 0.1 M pH 7.0 PBS at room temperature (25±2 °C). Inset: plot of electrocatalytic current versus H_2O_2 concentration at HCNTs-modified electrode.

stirring phosphate buffer solution (PBS; pH 7.0) at an applied potential of −0.4 V, the sensor responded rapidly to the substrate. The electrode achieved the maximum steady-state current within 4 s. The results clearly demonstrated that the electrocatalytic response was very fast. At pH 7.0, the linear range of the H_2O_2 sensor was from 0.5 to 115 μM, with a correlation coefficient of 0.9988 (inset in Figure 7), which is much wider than that (from 5 to 45 μM) of a reported biosensor.[40] The detection limit with a signal-to-noise ratio of three was estimated to be 0.12 μM, which is lower than the level of 1.4 μM reported for a $(PDDA/Fe_3O_4\ NPs)_5$ multilayer modified electrode.[41] For comparison, the amperometric responses of l-HCNTs/GCE and MWCNTs/GCE are shown in Figure 7(curves b and c). Upon the addition of H_2O_2, the reduction current again increased. Howev-

er, the catalytic responses were smaller than those at the HCNTs-modified GCE. By comparison, it can be concluded that HCNTs offered significant advantages over l-HCNTs and MWCNTs in terms of amperometric response to H_2O_2. The results were consistent with the observations of intrinsic peroxidase-like activity of HCNTs as shown in Figure 6.

The effects of temperature on the electrocatalytic activity of the HCNTs are shown in Figure 8a, in which the relative activity is defined as the ratio of the electrocatalytic response at a given condition to the maximum electrocatalytic response. Upon increasing the temperature of the detection solution from 10 to 70 °C, the electrocatalytic activity for the reduction of H_2O_2 first increased then decreased. The maximum catalytic activity was observed at approximately 40 °C.

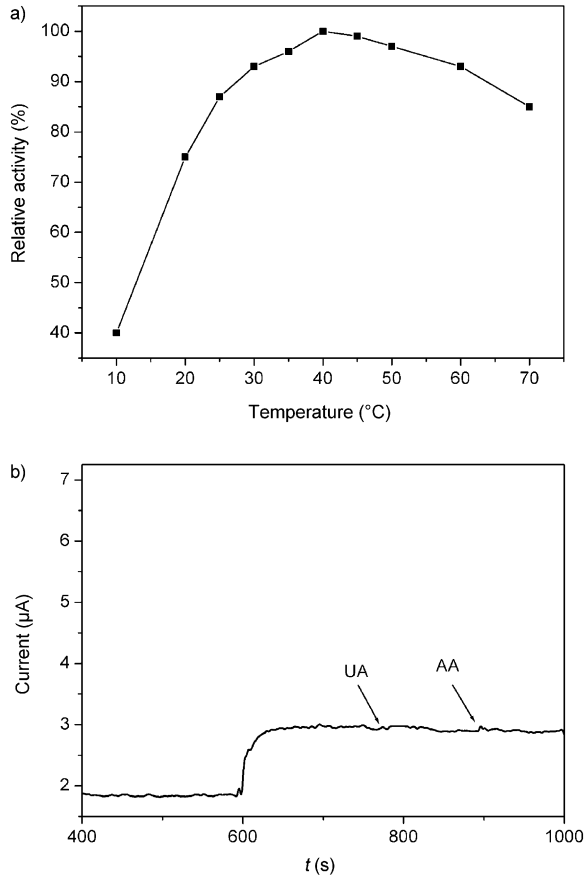

Figure 8. a) Effect of temperature on the electrocatalytic response of HCNTs to H_2O_2 reduction. b) Effect of interfering species on the sensor response with 10 μM of H_2O_2 in 0.1 M PBS (pH 7.0).

One of the outstanding advantages of HCNTs for the detection of H_2O_2 is their good stability, both thermal stability and long-term stability. Unlike the inherently unstable enzymes, the as-prepared HCNTs could maintain their high electrocatalytic ability either during high-temperature incubation or long-term storage. HCNTs were first incubated at 60 °C for 1 h and then the electrocatalytic reaction was performed at room temperature. Under these circumstances, the electrocatalytic current response was 93.0% of that without the incubation process. On the other hand, the long-term stability was also investigated over 60 days. After 60 days, the current response towards 0.5 mM H_2O_2 was maintained at 95.3% of the initial response when the sensor was stored at room temperature. The reproducibility of the sensor was assessed by performing measurements in 0.1 M PBS (pH 7.0). The relative standard deviation (RSD) of the sensor response to 10 μM H_2O_2 was 5.6% for seven successive measurements.

We investigated the interference effects of ascorbic acid (AA) and uric acid (UA) on the determination of H_2O_2. Specifically, the interfering effects of 100 μM AA and 100 μM UA compared to 10 μM H_2O_2 were evaluated at a potential of −0.4 V. As shown in Figure 8b, there was an obvious current response upon the addition of 10 μM H_2O_2. On the contrary, no obvious current responses were observed upon the addition of 100 μM AA and 100 μM UA, indicating that these species did not affect the determination of H_2O_2. The attractive performance of the proposed H_2O_2 sensor illustrated the advantage of the HCNTs-based "artificial peroxidase" as a transducer for H_2O_2 detection and the construction of reagentless amperometric biosensors.

Conclusion

A combined hydrothermal/hydrogen-reduction method has been developed for the mass production of HCNTs by the pyrolysis of acetylene at 475 °C in the presence of Fe_3O_4 NPs. The synthesized HCNTs were firstly found to exhibit attractive intrinsic peroxidase-like activity, which was confirmed by their ability to catalyze the oxidation of TMB by H_2O_2. Catalysis by HCNTs showed typical Michaelis–Menten kinetics, and the system exhibited high catalytic efficiency. This property of the HCNTs was exploited in the construction of an H_2O_2 sensor, which showed a more sensitive response than previously reported enzyme-based biosensors. Because of their low cost and high stability, these novel metallic HCNTs may represent a promising candidate as mimetic enzymes, and may find a wide range of new applications, such as in biocatalysis, immunoassay, and environmental monitoring.

Experimental Section

Materials and synthesis: Multi-walled carbon nanotubes (CNTs, CVD method, purity >95%, diameter 30–60 nm, length 0.5–15 μm) were purchased from Nanoport Co. Ltd. (Shenzhen, China). H_2O_2 (30%), $FeCl_3{\cdot}6H_2O$, sodium acetate, ethylene glycol, anhydrous ethanol, and sodium chloride were purchased from Shanghai Biochemical Reagent Company (China). Poly(allylamine hydrochloride) (PAH) ($M_w \approx 15000$) was purchased from Sigma–Aldrich. All chemicals and solvents were of analytical grade. All solutions were prepared with doubly distilled deionized water deoxygenated by bubbling highly pure nitrogen through it. 0.1 M phosphate buffer solutions of different pH were prepared by mixing stock standard solutions of Na_2HPO_4 and NaH_2PO_4 and adjusting the pH with 0.1 M H_3PO_4 or NaOH.

Synthesis of catalyst precursor: In a typical synthesis of monodisperse Fe_3O_4 NPs, $FeCl_3{\cdot}6H_2O$ (1.0 g) was dissolved in EG (20 mL) to form a clear solution, to which NaOAc (3.0 g), NaOH (0.8 g), and 1,2-ethylenediamine (ETH; 10 mL) were added. The mixture was stirred vigorously for 30 min and then sealed in a Teflon-lined stainless steel autoclave. The autoclave was heated to 200 °C and maintained at this temperature for 8 h, and then allowed to cool to room temperature. The obtained black magnetite particles were washed six times with ethanol and then dried in vacuum at 60 °C for 12 h.

Typical synthesis of HCNTs: Briefly, catalytic precursor powder (100 mg) was spread on a ceramic plate, which was placed in a quartz reaction tube (5 cm inner diameter and 35 cm in length). This assembly was laid in a stainless steel reaction tube of 5.2 cm inner diameter and 80 cm in length (equipped with temperature and gas-flow controls). The Fe_3O_4 NPs were reduced in H_2 at 425 °C for 4 h, and then acetylene decomposition was conducted at 475 °C for 1 h at atmospheric pressure in the presence of the Fe catalyst. After the system was cooled to room temperature, the as-prepared sample was obtained.

Preparation of soluble HCNTs and MWCNTs: The HCNTs were functionalized with PAH according to the following procedure: HCNTs were dispersed at 3 mg mL^{-1} in an aqueous solution of PAH (0.20 %; pH 7.0) containing NaCl (0.5 M) and the resulting dispersion was sonicated for 30 min to give a homogeneous black suspension. Residual PAH polymer was removed by magnetic separation and the complex was rinsed with water at least three times. The collected complex was redispersed in water with mild sonication to produce a stable solution.

MWCNTs were chemically shortened by ultrasonic agitation in a mixture of sulfuric acid and nitric acid (3:1) for 3 h. The resulting CNTs were separated and washed repeatedly with distilled water by centrifugation until the pH of the washings was about 7.

Preparation of HCNTs-modified electrode: A GCE of diameter 3 mm was used as the substrate to grow an HCNTs film. Prior to preparation of the film, the GCE was successively polished to a mirror finish using 0.3 and 0.05 μm alumina slurry (Beuhler) and then thoroughly rinsed with water. After successive sonications in 1:1 nitric acid/water, acetone, and doubly distilled water, the electrode was rinsed with doubly distilled water and allowed to dry at room temperature. HCNTs solution (4 μL of 3.0 mg mL^{-1}) was dropped onto the pretreated GCE and allowed to dry under ambient conditions for 3 h to obtain the HCNTs-modified electrode.

Apparatus and procedures: Field-emission scanning electron microscopy (FE-SEM) images were obtained by using a Hitachi S-4800 field-emission electron microscope operating at an accelerating voltage of 5 kV. Transmission electron microscopy (TEM) images and selected-area electron diffraction (SAED) patterns were obtained using a JEOL JEM-2010 transmission electron microscope operating at an accelerating voltage of 200 kV. Zeta potentials (ξ) of HCNTs and PAH-functionalized HCNTs were measured in pure water on a Malvern Nano-Z instrument. Static water contact angles were measured at 25 °C by means of a contact-angle goniometer (Rame-Hart-100) employing drops of pure water. The readings were allowed to stabilize and taken within 120 s of addition. Powder X-ray diffraction (XRD) data were collected on a Shimadzu XD-3A X-ray diffractometer ($Cu_{K\alpha}$ radiation, $\lambda = 0.15418$ nm). Magnetic measurements were carried out using a Lakeshore 7300 vibrating sample magnetometer (VSM) under a magnetic field of up to 10 kOe.

Peroxidase-like activity of HCNTs: Kinetic measurements of peroxidase reactions with HCNTs were performed on a Jasco-V550 UV/Vis spectrophotometer. The cell length of the colorimetric cuvette in the spectrophotometric method was 0.5 cm. Experiments were carried out by using HCNTs (40 μg mL^{-1}) in Na_2HPO_4 buffer (25 mM, reaction volume 500 μL), with TMB (800 μM) as the substrate. The H_2O_2 concentration was 500 mM, the pH was 4.0, and the temperature was 40 °C, unless otherwise stated. Catalytic parameters were determined by fitting the absorbance data to the Michaelis–Menten equation.[9]

$$v = \frac{v_{max}[S]}{K_m + [S]}$$

The Michaelis–Menten equation describes the relationship between the rates of substrate conversion by an enzyme and the concentration of the substrate. In this equation, v is the rate of conversion, v_{max} is the maximum rate of conversion, $[S]$ is the substrate concentration, and K_m is the Michaelis constant. The Michaelis constant is equivalent to the substrate concentration at which the rate of conversion is half of v_{max} and K_m approximates the affinity of the enzyme for the substrate.

Electrocatalytic activity of HCNTs in the reduction of H_2O_2: Amperometric measurements were performed on a CHI 660 apparatus (CHI, USA). A three-electrode system comprising a platinum wire as auxiliary, a saturated calomel electrode as reference, and the HCNTs-modified electrode as the working electrode was used for all electrochemical experiments. The experiments were carried out in a cell containing PBS (15.0 mL of 0.1 M) at room temperature (25 ± 2 °C). All solutions were deoxygenated by bubbling highly pure nitrogen through them for at least 15 min and were maintained under nitrogen atmosphere during the measurements. In the amperometric experiments, current–time data were recorded after a constant residual current was established and successive additions of H_2O_2 solution to the buffer were completed. Experiments were carried out by applying a potential of −0.4 V across a stirred cell at room temperature. The sensing response was measured as the difference between the total and residual currents.

Acknowledgements

This work has been supported by the National Natural Science Foundation of China (Grant Nos. 20905010, 51001019, 20821063), the National Basic Research Program of China (2011CB933502), and the China Postdoctoral Science Foundation (Project No. 20100471293).

[1] C. X. Yu, J. Irudayaraj, *Anal. Chem.* **2007**, *79*, 572–579.
[2] X. H. Huang, I. H. El-Sayed, W. Qian, M. A. El-Sayed, *Nano Lett.* **2007**, *7*, 1591–1597.
[3] Z. H. Wen, Q. Wang, J. H. Li, *Adv. Funct. Mater.* **2008**, *18*, 959–964.
[4] Z. H. Wen, S. Q. Ci, J. H. Li, *J. Phys. Chem. C* **2009**, *113*, 13482–13487.
[5] H. D. Hill, R. A. Vega, C. A. Mirkin, *Anal. Chem.* **2007**, *79*, 9218–9223.
[6] S. Boland, F. Barriere, D. Leech, *Langmuir* **2008**, *24*, 6351–6358.
[7] a) X. B. Lu, J. H. Zhou, W. Lu, Q. Liu, J. H. Li, *Biosens. Bioelectron.* **2008**, *23*, 1236–1243; b) X. B. Lu, Z. H. Wen, J. H. Li, *Biomaterials* **2006**, *27*, 5740–5747.
[8] P. Zhou, Z. Dai, M. Fang, X. Huang, J. Bao, *J. Phys. Chem. C* **2007**, *111*, 12609–12616.
[9] L. Gao, J. Zhuang, L. Nie, J. B. Zhang, Y. Zhang, N. Gu, T. H. Wang, J. Feng, D. L. Yang, S. Perrett, X. Y. Yan, *Nat. Nanotechnol.* **2007**, *2*, 577–583.
[10] H. Wei, E. K. Wang, *Anal. Chem.* **2008**, *80*, 2250–2254.
[11] Y. Song, X. Wang, C. Zhao, K. Qu, J. Ren, X. Qu, *Chem. Eur. J.* **2010**, *16*, 3617–3621.
[12] A. Asati, S. Santra, C. Kaittanis, S. Nath, J. M. Perez, *Angew. Chem.* **2009**, *121*, 2344–2348; *Angew. Chem. Int. Ed.* **2009**, *48*, 2308–2312.
[13] Z. Dai, S. Liu, J. Bao, H. Ju, *Chem. Eur. J.* **2009**, *15*, 4321–4326.
[14] S. Itoh, S. Ihara, J. Kitakami, *Phys. Rev. B* **1993**, *47*, 1703–1704.
[15] S. Amelinckx, X. B. Zhang, D. Bernaerts, X. F. Zhang, V. Ivanov, J. B. Nagy, *Science* **1994**, *265*, 635–639.
[16] X. B. Zhang, X. F. Zhang, D. Bernaerts, G. Van Tendeloo, S. Amelinckx, J. V. Landuyt, V. Vanov, J. B. Nagy, P. Lambin, A. A. Lucas, *Euro. Phys. Lett.* **1994**, *27*, 141–147.
[17] A. Volodin, M. Ahlskog, E. Seynaeve, C. Haesendonck, A. Fonseca, J. B. Nagy, *Phys. Rev. Lett.* **2000**, *84*, 3342–3345.
[18] X. Q. Chen, S. L. Zhang, D. A. Dikin, W. Q. Ding, R. S. Ruoff, L. J. Pan, Y. Nakayama, *Nano Lett.* **2003**, *3*, 1299–1304.
[19] V. Bajpai, L. M. Dai, T. Ohashi, *J. Am. Chem. Soc.* **2004**, *126*, 5070–5078.

[20] J. N. Xie, K. Mukhopadyay, J. Yadev, V. K. Varadan, *Smart Mater. Struct.* **2003**, *12*, 744–748.
[21] A. Volodin, D. Buntinx, M. Ahlskog, A. Fonseca, J. B. Nagy, C. Van Haesendonck, *Nano Lett.* **2004**, *4*, 1775–1779.
[22] N. J. Tang, W. Zhong, C. T. Au, A. Gedanken, Y. Yang, Y. W. Du, *Adv. Funct. Mater.* **2007**, *17*, 1542–1550.
[23] R. Cui, C. Liu, J. Shen, D. Gao, J.-J. Zhu, H.-Y. Chen, *Adv. Funct. Mater.* **2008**, *18*, 2197–2204.
[24] X. X. Yan, D.-W. Pang, Z.-X. Lu, J.-Q. Li, H. Tong, *J. Electroanal. Chem.* **2004**, *569*, 47–51.
[25] J. Wang, M. Musameh, Y. Lin, *J. Am. Chem. Soc.* **2003**, *125*, 2408–2409.
[26] M. D. Rubianes, A. R. Gustavo, *Electrochem. Commun.* **2007**, *9*, 480–484.
[27] C. H. Song, P. E. Pehrsson, W. Zhao, *J. Phys. Chem. B* **2005**, *109*, 21634–21639.
[28] L. Gao, Q. Gao, *Biosens. Bioelectron.* **2007**, *22*, 1454–1460.
[29] J.-J. Feng, J.-J. Xu, H.-Y. Chen, *Electrochem. Commun.* **2006**, *8*, 77–82.
[30] S. Guo, D. Li, L. Zhang, J. Li, E. K. Wang, *Biomaterials* **2009**, *30*, 1881–1889.
[31] N. Tang, J. Wen, Y. Zhang, F. Liu, K. Lin, Y. Du, *ACS Nano* **2010**, *4*, 241–250.
[32] T. Luo, J. W. Liu, L. Y. Chen, S. Y. Zeng, Y. T. Qian, *Carbon* **2005**, *43*, 755–759.
[33] J. N. Wang, L. F. Su, Z. P. Wu, *Cryst. Growth Des.* **2008**, *8*, 1741–1747.
[34] E. I. Karaseva, Y. P. Losev, D. I. Metelitsa, *Russ. J. Bioorg. Chem.* **2002**, *28*, 128–135.
[35] X. Q. Zhang, S. Gong, Y. Zhang, T. Yang, C. Wang, N. Gu, *J. Mater. Chem.* **2010**, *20*, 5110–5116.
[36] O. Wolfbeis, A. Dürkop, M. Wu, Z. Lin, *Angew. Chem.* **2002**, *114*, 4681–4684; *Angew. Chem. Int. Ed.* **2002**, *41*, 4495–4498.
[37] J. Jia, B. Wang, A. Wu, G. Cheng, Z. Li, S. Dong, *Anal. Chem.* **2002**, *74*, 2217–2223.
[38] J. Lin, L. Zhang, S. Zhang, *Anal. Biochem.* **2007**, *370*, 180–192.
[39] G. Zou, H. Ju, *Anal. Chem.* **2004**, *76*, 6871–6876.
[40] W. Y. Cai, L. D. Feng, S. H. Liu, J. J. Zhu, *Adv. Funct. Mater.* **2008**, *18*, 3127–3136.
[41] L. Zhang, Y. Zhai, N. Gao, D. Wen, S. Dong, *Electrochem. Commun.* **2008**, *10*, 1524–1533.

Received: February 12, 2011
Published online: July 18, 2011

